Dalton Transactions

Accepted Manuscript

ROYAL SOCIETY OF CHEMISTRY

www.rsc.org/dalton

Journal Name

RSCPublishing

ARTICLE

Neocarzinostatin-Based Hybrid Biocatalysts for Oxidation Reactions

Cite this: DOI: 10.1039/xoxxoooooox

Elodie Sansiaume-Dagousset [a], Agathe Urvoas [b], Kaouthar Chelly [a], Wadih Ghattas[a], Jean-Didier Maréchal [c], Jean-Pierre Mahy*[a] and Rémy Ricoux*[a]

Received ooth January 2012,
Accepted ooth January 2012

DOI: 10.1039/xoxxoooooox

www.rsc.org/

An anionic iron(III)-porphyrin–testosterone conjugate 1-Fe has been synthesized and fully characterized. It has been further associated to a neocarzinostatin variant, NCS-3.24, to generate a new artificial metalloenzyme following the so-called 'Trojan Horse' strategy. This new 1-Fe-NCS-3.24 biocatalyst showed an interesting catalytic activity as it was found able to catalyze the chemoselective and slightly enantioselective (ee = 13 %) sulfoxidation of thioanisole by H_2O_2. Molecular modelling studies show that a synergy between the binding of the steroid moiety and that of the porphyrin macrocycle into the protein binding site can explain the experimental results indicating a better affinity of 1-Fe for the NCS-3.24 variant than testosterone and testosterone-hemisuccinate themselves. They also show that the Fe-porphyrin complex is sandwiched between the two subdomains of the protein providing with good complementarities. However, the artificial cofactor entirely fills the cavity and the its metal ion remains widely exposed to the solvent which explains the moderate enantioselectivity observed. Some possible improvements of the "Trojan horse" strategy for obtaining better catalysts of selective oxidations are presented.

Introduction

The synthesis of enantio-pure compounds is a major issue in organic chemistry, especially in pharmaceutical chemistry, as it is well known that the two enantiomers of chiral products can possess different biological activities. One of the most efficient ways to obtain such products, which is both cost-effective and eco-friendly, is asymmetric catalysis that uses low quantities of chiral catalysts. Among those, a promising new kind of eco-compatible hybrid biocatalysts, that combine the advantages of both biocatalysis and homogeneous catalysis, has recently been developed: artificial metalloenzymes or « Artzymes ».[1] Such catalysts associate a synthetic metal-cofactor that is responsible for the catalytic activity with a protein that provides the metal cofactor with a chiral environment and protects it against degradation. They are not only able, like enzymes, to work under mild conditions with a high stereoselectivity, but they can also be used in a wide scope of reactions like synthetic catalysts. Additionally, their efficiency and selectivity can be optimized both on the protein side, by directed evolution, and on the metal cofactor side by chemical modification of the ligand.

Different strategies have been described to obtain artzymes. First, the direct insertion of a metal ion into proteins has led to systems able to catalyze various reactions such as selective bis-hydroxylation and hydroformylation of alkenes, sulfoxidation of sulphides, epoxidation of styrene derivatives, Diels-Alder reactions.[2-6] Alternatively, the modification of the coordination sphere of the metal ion in metalloenzymes has been used to drive the stereoselectivity of hydroxylation reactions.[7] Second, other metalloenzymes have been obtained upon the covalent attachment of a metal cofactor into a protein, most often by a covalent bond with a cysteine residue, and have been used to catalyze a wide range of enantioselective transformations such as hydrolysis of esters, sulfoxidation, epoxidation, hydrogenation and Diels Alder reaction.[7-12] Finally, artzymes can also been obtained after the supramolecular anchoring of metal cofactors into proteins, using either the "host-guest strategy" or the "Trojan-horse strategy". The former was used to generate artzymes that catalyzed the stereoselective sulfoxidation of thioanisole[14,15], the stereoselective Diels-Alder reaction[16] or dihydrogen production[17] or that displayed an peroxidase activity[18] and O_2 binding properties.[19] We ourselves prepared by non-covalent insertion of iron- and manganese- anionic tetraarylporphyrins in xylanase A artificial hemoproteins that were found able to catalyze the stereoselective sulfoxidation of thioanisole by H_2O_2[20] and epoxidation of styrene derivatives by oxone.[21] The "Trojan-horse strategy" was historically introduced by Whitesides and coworkers but mainly developed and optimized by Ward *et al.* Taking advantage of the strong affinity between streptavidin and biotin, a biotinylated transition metal complex are inserted into streptavidin and its variants to build new artificial metalloenzymes that were able to catalyze the stereoselective reduction of acetamido-acrylic acid by H_2.[22,23]

We also previously used the "Trojan-horse strategy" to build new artificial hemoproteins. Taking advantage of the strong affinity of a

monoclonal antibody for its anti-estradiol antigen (K_d = 9.5 x 10^{-10}M), the artificial hemoproteins were built by insertion of Fe- or Mn-porphyrin-estradiol conjugates into the anti-oestradiol antibody.[24-26] These biocatalysts catalyze selective oxidations such as the enantioselective sulfoxidation of thioanisole by H_2O_2 with a 10% enantiomeric excess and the chemoselective epoxidation of styrene by $KHSO_5$. However, in the later case, no enantiomeric excess was observed. We thus decided to improve these selectivities by turning towards another protein. In particular, we focused on the neocarzinostatin (NCS), a 113 amino-acid protein that is the most studied member of a family known as chromoproteins, secreted by *Streptomyces*. Each member of this family tightly and specifically binds a nine membered enediyne "chromophore" that is responsible for the powerful cytotoxic and antibiotic activities of the chromoprotein complexes. It has thus been intensively studied for its antitumor properties and has also been engineered as a potential drug-carrying scaffold.[27-30] In a previous study, the ligand-binding pocket of NCS was remodeled and directed evolution techniques were used to create a new binding site for a target unrelated to its natural ligand. In particular, the NCS-3.24 variant, that contains 7 mutations in the binding site : D33W, G35A, C37W, W39R, L45W, C47Y and F52N, with respect to wild type NCS, was found to bind testosterone with a good affinity (K_d = 13 x 10^{-6} M) and its X-ray structure was solved in the apo and complexed forms.[29] We thus decided to associate this NCS variant with an iron(III)-tetrarylporphyrin-testosterone conjugate **1-Fe**. We here present the synthesis of this new metalloporphyrin-testosterone conjugate, as well as the characterization of its complex with the NCS-3.24 variant and its catalytic activity in the oxidation of thioanisole by H_2O_2.

Our results show that these new biocatalysts have an interesting catalytic activity in oxidation reactions. The iron(III)–anionic-porphyrin–testosterone-NCS variant complex was found able to catalyze the chemoselective and enantioselective (ee = 13%) oxidation of thioanisole into sulfoxide by H_2O_2. Molecular modelling studies showed that the Fe-porphyrin complex was sandwiched between the two sides of the protein cavity occupying most of the available space of the binding region, hence providing a chiral environment around the iron atom. Moreover, the nearby environment of the iron remained exposed to the solvent. Both elements could explain the moderate enantioselectivity observed.

Results and Discussion

Synthesis of iron(III)-5,10,15-tris(4-sulfonatophenyl)-20-(17'-succininimidyl-testosterone) porphyrin 1-Fe.

5,10,15-tris(4-sulfonatophenyl)-20-(4phenyl(17'-succininimidyl-testosterone))porphyrin ($TpSPpNHSucTestoPPH_2$) **1** was first synthetized in three steps (Scheme 1). 17'-succininimidyl-testosterone was first synthetized by a method described previously by Hong Xu Chen and Xin Xiang Zhang.[31] The 17'-OH function of commercially available testosterone was thus esterified by succinic anhydride in the presence of pyridine under inert atmosphere as described in materials and methods to lead to 17'-succininimidyltestosterone with 72% yield. The product was characterized by NMR and MALDI-ESI spectroscopies that were in agreement with the expected structure.

Then, the acidic function of the modified steroid was engaged in a peptide coupling reaction with the amino group of the meso-para-aminophenyl substituent of the para-sulfonatophenyl substituted porphyrin $TpSPpNH_2PPH_2$, that had been prepared as described previously.[26,32,33] The best result was obtained with isobutyl chloroformate as the coupling agent in the presence of *N*-methylmorpholine as the base. Owing to the high solubility of the obtained porphyrin **1** in water, purification was not easy and required several steps including extensive washings of the water phase by dichloromethane in order to remove the excess of testosterone and two final successive purifications on a H^+ cation exchange column first and, second, on a Na^+ column AG-50W-X8. After lyophilisation, porphyrin **1** was obtained as a purple solid in a 24% yield. It was characterized by NMR and MALDI-ESI spectroscopies that were in agreement with the expected structure.

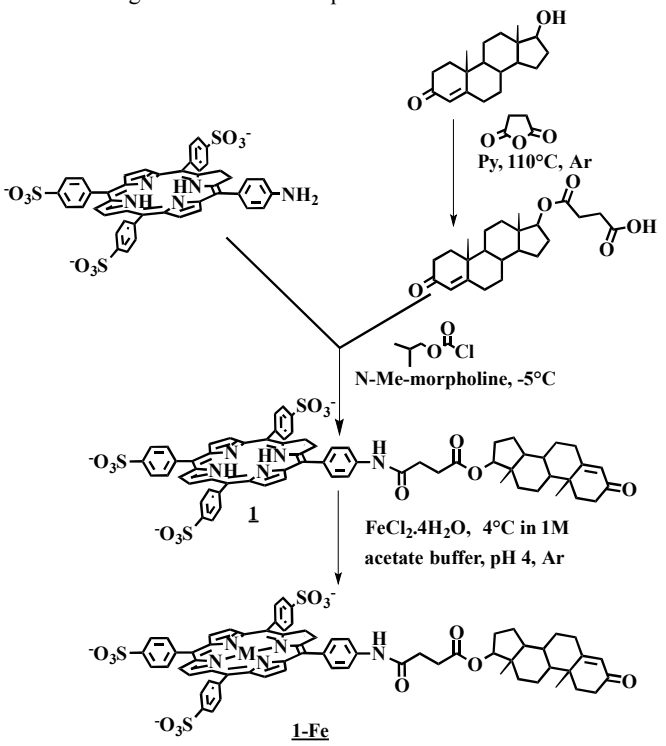

Scheme 1. Synthesis of the iron(III)-5,10,15-tris(4-sulfonatophenyl)-20-(17'-succininimidyl-testosterone) porphyrin **1-Fe**.

1-Fe was prepared following a classical protocol described by Fleischer et al.[34] upon reaction of porphyrin **1** with excess $FeCl_2.4H_2O$ at 4°C in 1M acetate buffer, pH 4 under inert atmosphere. After solvents removal, the water-soluble metalloporphyrin was dissolved in water and purified on a Na^+ cation exchange column (AG-50W-X8). **1-Fe** was obtained after lyophilisation as a dark purple solid in a 95% yield.

Insertion of 1-Fe in the cavity of the NCS-3.24 variant.

The UV-spectrum of a 5 µM solution of **1-Fe** was recorded twice in 50 mM citrate-phosphate buffer, pH 4, alone or in the presence of a slight excess of the NCS-3.24 protein (1.2 equiv.), in order to favour the binding of the testosterone moiety inside its binding site (Fig. 1). When comparing the spectra of **1-Fe** and that of NCS-3.24-**1-Fe** (Fig. 1), it appears that the binding of **1-Fe** into NCS-3.24 causes a slight 4 nm shift of the Soret band, from 412 to 416 nm, accompanied by an increase of its intensity, and a slight 5 nm shift of the Q band, from 540 to 545 nm (Table 1) together with a decrease of its intensity. It is thus clear that the presence of the protein slightly influences the shape of the UV-Vis spectrum of **1-Fe**, with rather slight modifications that are in agreement a change of the hydrophobicity of the environment of the porphyrin.[35] This clearly testifies of an interaction between the cofactor and the protein. The 4 nm shift of the Soret band, accompanied by the 5 nm shift of the Q-band could also be the sign of the coordination of a weak ligand coming from one amino acid side chain of the protein on one face of the iron.

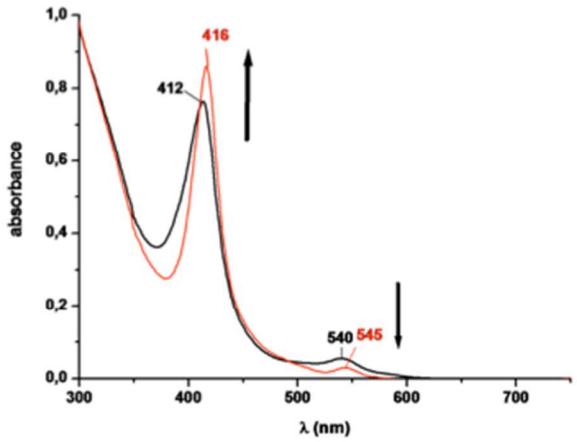

Figure 1. Comparison of the UV-visible spectra of 5 □M **1-Fe** and NCS-3.24-**1-Fe** in 50 mM citrate-phosphate buffer, pH 4.

Table 1. UV-visible characteristics of metalloporphyrin-testosterone cofactor **1-Fe,** and its complex with NCS-3.24 variant.

Complex	UV-visible characteristics λ_{max}(nm) (ε($M^{-1}cm^{-1}$))	K_D (μM)
1-Fe	412 (1.52 x 10^5), 540	-
1-Fe-3-24	416 (1.72 x 10^5), 545	1.6

In order to determine the dissociation constant of the corresponding NCS-3.24-**1-Fe** cofactor complex, increasing amounts, from 0 to 10 μM, of NCS-3.24 variant were added respectively to a 5 μM solution of **1-Fe** in 50 mM citrate-phosphate buffer, pH 4. The titration was followed by UV-visible spectroscopy as described in the experimental section. The difference between the absorbance at 412 nm of **1-Fe** and that of **1-Fe**-NCS-3.24 (ΔA_{412} = $A_{\underline{1\text{-Fe}}}$ − $A_{\underline{1\text{-Fe}}\text{-NCSv}}$) was plotted against the metal cofactor/NCS variant ratio. It has previously been reported[19b] that ΔA could be related to the dissociation constant K_D by the following relation:

$$[S]_0 = \frac{\Delta A}{\varepsilon_{\underline{1\text{-Fe}}} - \varepsilon_{\underline{1\text{-Fe}}\text{-NCSv}}} \bullet \left(1 + \frac{K_D}{[\underline{1\text{-Fe}}]_0 - \frac{\Delta A}{\varepsilon_{\underline{1\text{-Fe}}} - \varepsilon_{\underline{1\text{-Fe}}\text{-NCSv}}}}\right) = g\left(\frac{\Delta A}{\varepsilon_{\underline{1\text{-Fe}}} - \varepsilon_{\underline{1\text{-Fe}}\text{-NCSv}}}\right)$$

As a result, K_D could be estimated with a non-linear regression of the initial concentration of NCS variant $[S]_0$ with the function g (ΔA / $\varepsilon_{\underline{1\text{-Fe}}}$ − $\varepsilon_{\underline{1\text{-Fe}}\text{-NCSv}}$). It then appears that NCS-3.24 was able to bind the iron(III) hydrosoluble porphyrin linked to testosterone through a succinimidyl arm, **1-Fe** with a K_D constant in the micromolar range. Indeed, a K_D value of about 1.6 μM could be determined for the dissociation constant of the **1-Fe**-NCS-3.24 complex (Table 1).

The binding of iron(III)-tetra-p-sulfonato-phenylporphyrin **TpSPP-Fe** by NCS-3.24 was also examined in order to appreciate the contribution of the porphyrinic ring to the binding of **1-Fe** in the binding site of this protein. A K_D value of 12.5 μM was found for the Fe(III)-TpSPP-NCS-3.24 complex.

These values can be compared with those previously reported by Minard *et al.* who showed that NCS-3.24[29] was able to bind testosterone as well as testosterone-hemisuccinate (THS). This constitutes a shortened charged form of the spacer arm of biotinylated testosterone that was used during the selection of the NCS variants and also constitutes the non-porphyrinic part of **1**. Fluorescence titration experiments allowed the determination of the dissociation constants for the NCS-3.24-testosterone complex, K_D = 13 μM and for the NCS-3.24-THS complex K_D = 40.15 μM.[29] Since the K_D values determined here for the **1-Fe**-variant complexes were in the micromolar range (Table 1), it is clear that the covalent attachment of the succinimidyl-testosterone arm to the porphyrin does not prevent the binding of the testosterone moiety inside the cavity of the NCS-3.24 variant but it even improves its binding properties.

Taking into account that NCS-3.24 also binds Fe-TpSPP with a K_D of 12.5 μM, it is then clear that a synergetic effect between the binding of the testosterone moiety and that of the porphyrinic ring leads to a better association of **1-Fe** with NCS-3.24 than that of both testosterone and THS alone.

In order to get a deeper insight on the molecular grounds that govern the interaction of **1-Fe** with the NCS variant, molecular modelling was performed.

Molecular modelling studies of the interaction of 1-Fe with the NCS-3.24 variant.

Despite several experimental structures of neocarzinostatin are available in the Protein Data Bank, only one corresponds to the NCS-3.24 protein (pdb code 2cbo). In this structure, the testerone hemisuccinate used for our Trojan horse strategy is bound simultaneously at two different sites at the flanks of the protein cavity creating a relatively large but solvent exposed region for the binding of chemicals.

Because of the relevance for our dockings to reproduce as accurately as possible the binding of steroids to the NCS-3.24 variant, a first part of our computational study was dedicated to benchmark the scoring functions available in GOLD in reproducing the X-ray structure of the NCS-3.24/THS complexes. Dockings were performed with all the scoring functions available in GOLD (ASP, ChemScore, GoldScore and ChemPLP) and the resulting low energy binding modes compared with the experimental structure. In all calculations, the binding modes at both sites were predicted to be almost isoenergetic, something consistent with the characterization of simultaneous bindings in the X-ray structure. However, amongst the 20 docking solutions, a wide ensemble of conformations were observed, a situation consistent with the dominant hydrophobic nature of the complementarity between the ligands and the protein as well as the wide solvent access of the steroid binding sites. Calculations ultimately showed that GoldScore was the most efficient in reproducing the structural features of the testosterone hemisuccinate leading to good agreements between theoretical and experimental complexes. Hence, GoldScore was used in the remaining part of the work.

The second part of the study was dedicated to the prediction of the low energy binding modes of the iron(III)-tetra-para-sulfonatophenylporphyin **TpSPP-Fe** into the NCS cavity. Dockings were carried out using the same protocol as previously described (see Material and Methods). All 20 solutions were extremely similar one to the others with the lowest binding mode energy reaching 64.7 GoldScore units (Table 2).

Table 2. GoldScore scoring and breakdowns of the chemicals under investigation in this work.

Chemical	Fitness[a]	S_{hbond} [b]	S_{vdw} 4[c]]	$S_{hbond\ int}$[d]
Steroid	54.2	7.63	38.1	0.0
Porphyrin	64.7	19.9	36.3	0.0
Best Trojan	72.9	6	52.3	0.0

[a] Total GoldScore values and the most important terms contributing to them (dimensionless) [b] Protein-ligand hydrogen bonds [c] Protein-ligand hydrophobic contacts [d] ligand intramolecular hydrogen bonds

In this binding mode, the porphyrin presents a strong hydrophobic complementarity with the protein with most of the macrocycle well incorporated in the NCS cavity (Figure 2). The different quadrants of the porphyrin present several kinds of π–π interactions with tryptophan 37 and 33, phenylalanine 78 and tyrosine 47 (Figure 2). Additionally, two of the four sulfonates present a series of polar interactions with residues at the two extremities of the binding sites of NCS-3.24. This includes interactions with the nitrogen atom of the side chain of Gln 94 and the backbone nitrogen of Gly 107 on one side, the nitrogen atom of the side chain of Asn 52 and Trp 33 as well as the hydroxyl group of Tyr 47 on the other. The two remaining sulfonates are remaining widely exposed to the solvent.

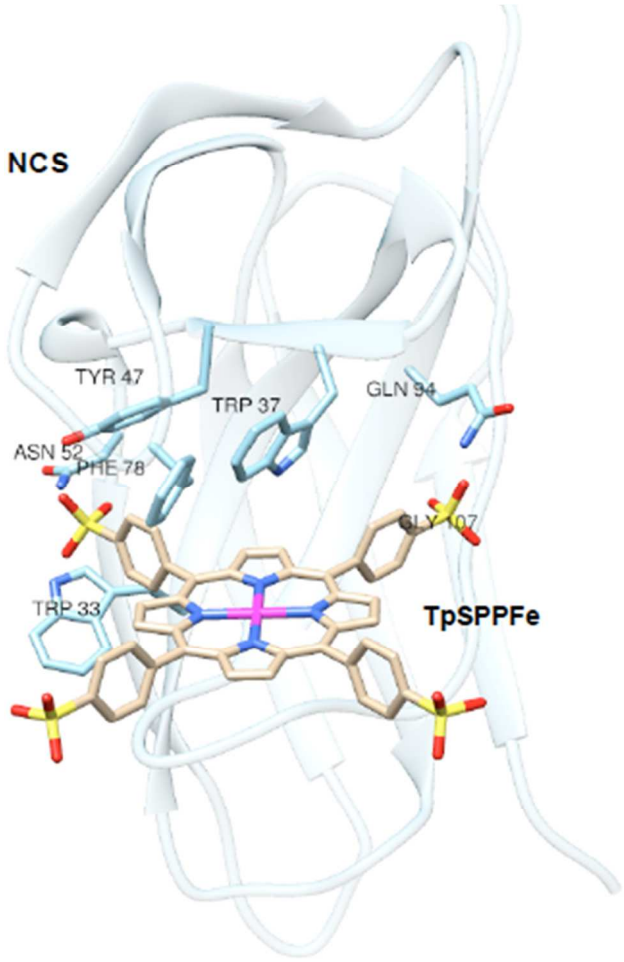

Figure 2. Representation of the lowest energy solution of the docking of unsubstituted porphyrin in the experimental structure of NCS-3.24 (pdb code 2cbo). The protein is represented in transparent cyan ribbons. Ligands and important residues of the binding site are represented in stick.

The calculated binding orientations of the porphyrin non-substituted by a 4-phenyl(17'-O-succinimidyltestosterone) arm present interesting comparisons with the native NCS-3.24/THS complex (Figure 3). On one side, the aromatic ring of **Fe-TpSPP** presents overlapping hydrophobic regions with the two testosterone moieties in their corresponding binding sites. On the other, the polar interactions of two of the para-sulfonate substituents of **Fe-TpSPP** almost perfectly match those of the carbonyl groups of both testosterone derivatives present in the original structure. In summary, the docking performed in this part of the study clearly shows that the unsubstituted porphyrin already presents relatively good complementarities with the NCS variant thanks to similar hydrophobic and polar patterns generated by about two thirds of the macrocycle with respect to two additive steroids. This general behaviour is in agreement with the experimental observation and suggests that porphyrinic scaffolds are viable candidates for providing NCS with peroxidase activity.

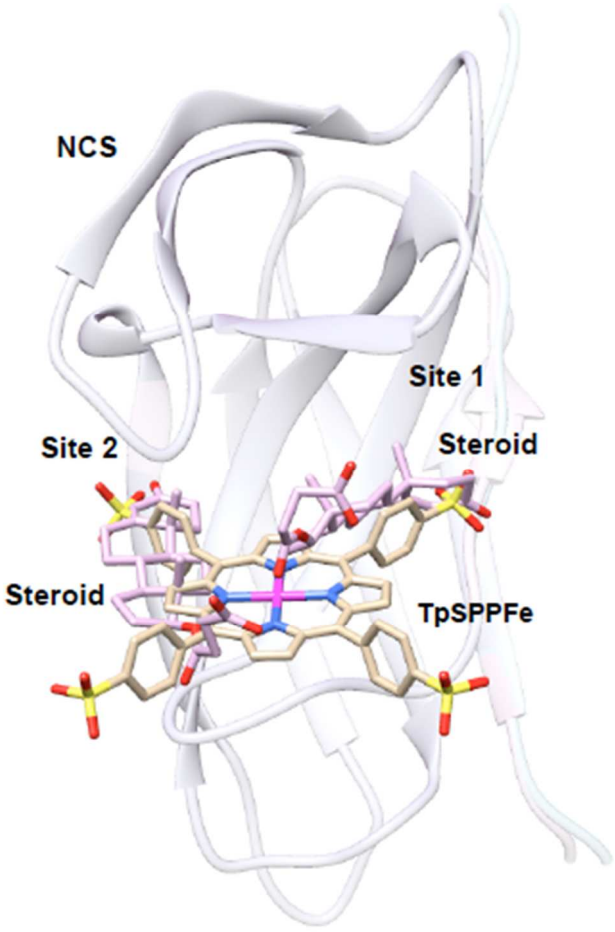

Figure 3. Representation of the lowest energy solution of the docking of unsubstituted porphyrin in the experimental structure of NCS-3.24 (pdb code 2cbo) in comparison with the experimentally characterized ligands. The protein is represented in transparent cyan ribbons and chemicals in stick. The porphyrin is colored in gold and the steroids in pink.

Finally, the calculations were carried out to predict low energy solution of the binding of the **1-Fe** "Trojan-horse" to the NCS-3.24 engineered NCS. Lowest energy solutions have scores close to 73 units, an improvement of 10 scoring units with respect to the naked porphyrin; something in line with the experimental observations. However, as a consequence of the wide exposure of the NCS binding site and the large dimension of the steroid conjugated porphyrin, the predicted structures of the complex present a large structural variability. This actually leads to three lowest energy solutions with less than 1.5 GoldScore units of difference and it would be presumptuous to simplify the discussion on one unique binding mode. Therefore, we here comment on the general features that these binding modes share and illustrate them with one of their solutions (Figure 4).

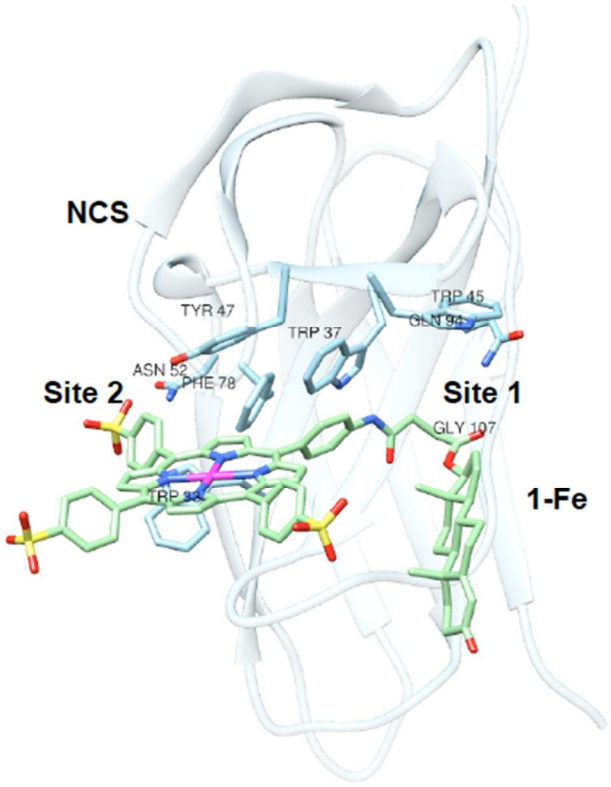

Figure 4. Representation of the lowest energy solution for the docking of **1-Fe** in the experimental structure of NCS-3.24 (pdb code 2cbo). The protein is represented in transparent cyan ribbons. Ligands and important residues of the binding site are represented in stick.

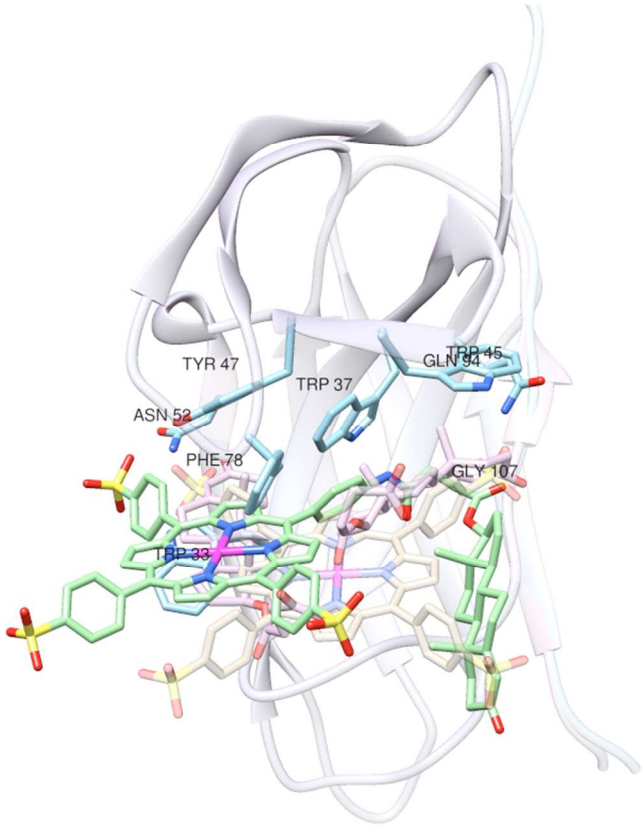

Figure 5. Representation of the lowest energy solution of the docking of **1-Fe** (in green) in the experimental structure of NCS-3.24 (pdb code 2cbo) in comparison with testosterone (in pink) and unsubstituted porphyrin (in gold). The protein is represented in transparent cyan ribbons. Ligands and important residues of the binding site are represented in stick and are colored in cyan.

In the lowest energy GOLD solutions, the porphyrin moiety of the homogenous catalyst is sandwiched between the two subdomains of the protein like in the previously reported experimental and calculated structures (Figure 4). The porphyrinic core presents important hydrophobic interaction with the same residues as those of the isolated porphyrin (Trp 37, Phe 78, Trp 45, Trp 33 and Tyr 47). Polar interactions are also observed with Gln 94, Gly 107, Asn 52 and Trp 33, Tyr 47. However, the two regions of **1-Fe** that are deeper anchored into the cavity of NCS-3.24 correspond to one of the sulfonated phenyl groups and the one holding the linker toward the steroid. This way, two sulfonates are systematically predicted to be in a solvent exposed medium, which, in turn, is consistent with a preference of ionic groups to stand in a hydrophilic environment with respect to hydrophobic and polar moieties. Possible coordination between the metal and the backbone carbonyl of the phenylalanine Phe 78 is also predicted (distance of ca. 3.5 Å).

Inside the binding site, neither the porphyrin nor the steroid maintains the same binding geometry as when docked separately. The porphyrin is slightly displaced perpendicularly to the main axis of the NCS then occupying more intensively one of the two sites of the steroids of the native X-ray structure. The testosterone moiety is also displaced with its atoms only partially occupying one of its original binding site and mainly packing to its outer region. Such changes are a consequence of the linker occupying most of the room of the steroid sites and its amide group actually forming a hydrogen bond with one of the polar patches on the testosterone cavities (Gln94/Gly107 and Asn52/Trp33/Tyr47 – Figure 5). The only differences between the lowest energy solutions depend on which of the two sub-cavities of the NCS occupies the chemical groups.

Sulfoxidation of thioanisole by H_2O_2 catalyzed by the 1-Fe-NCS-3.24 variant complex.

The influence of the NCS protein on the efficiency and on the selectivity of oxidation reactions catalyzed by the testosterone-iron(III)-porphyrin cofactor **1-Fe** was then studied. For this, the oxidation of thioanisole by H_2O_2 was performed as this substrate is well known as a typical substrate to be oxidized into an asymmetric sulfoxide by naturally occurring peroxidases like horseradish peroxidase (HRP),[36] which makes it a perfect candidate for a study of the enantioselectivity of the catalysis.

Only Fe-porphyrin-catalysts may be used for this reaction as it was previously shown[37] that Mn-porphyrin complexes were unable to catalyse the oxidation of thioanisole by H_2O_2 but instead lead to a catalase reaction. The sulfoxidation of thioanisole by H_2O_2 in the presence of 5 µM **1-Fe** alone or in the presence of 7.5 µM NCS-3.24 neocarzinostatin variant as catalyst and imidazole as co-catalyst, was thus carried out in 50 mM citrate-phosphate buffer, pH 4 under the following conditions: H_2O_2/thioanisole/imidazole/catalyst = 500/500/10/1, as described in Materials and Methods. After 2 hours, the organic products were extracted with ethyl acetate and analyzed by GC using benzophenone as the internal standard to determine the degree of conversion of the sulfide. Afterwards, chiral HPLC on a Chiracel OD-H column was used to determine the enantiomeric excess of the sulfoxide obtained.

In the absence of catalyst, no product coming from the oxidation of thioanisole was formed but, when the reaction was performed in the presence of either **1-Fe** or the bio-hybrid complex **1-Fe**-NCS-

3.24, the chemoselective formation of sulfoxide was observed with no trace of the corresponding sulfone (Scheme 2).

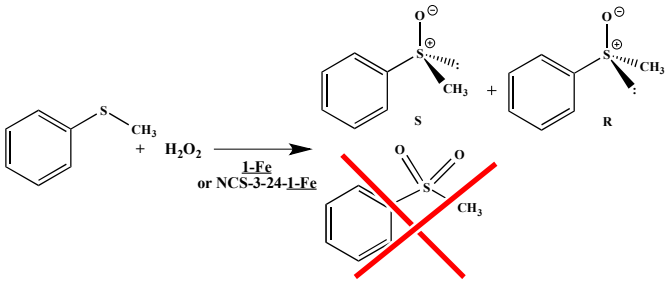

Scheme 2. Oxidation of thioanisole by H_2O_2 catalyzed by **1-Fe** and **1-Fe**-NCS-3.24 variant complexes.

In the absence of protein, 39 µM sulfoxide was formed, whereas 32 µM was obtained in the presence of NCS-3.24 (Table 3). This slight decrease could be due to a lower substrate accessibility to the iron when **1-Fe** is anchored to the binding site of NCS-3.24. Then, the reaction mixture was analyzed by chiral HPLC, and an enantiomeric excess of 13 % in favour of the *S*-enantiomer of the sulfoxide was obtained when **1-Fe**-NCS-3.24 was used as catalyst, whereas in the presence of only **1-Fe** as catalyst the racemic sulfoxide was obtained. This result thus confirmed that the protein environment influenced the enantioselectivity of the reaction.

Table 3. Amount of sulfoxide obtained after oxidation of thioanisole by H_2O_2 catalyzed by **1-Fe** and its complex with the NCS-3.24 variant in 50 mM citrate-phosphate buffer, pH 4 at RT.

Complex	Sulfoxide (µM)[a]	ee (%)	Configuration
1-Fe	39	-	-
1-Fe-3-24	32	13	S

[a] Conditions as in materials and methods: H_2O_2/thioanisole/imidazole/ catalyst = 500/500/10/1.

Indeed, as shown by the molecular modelling experiments, when inserted into the binding cavity of the NCS-3.24 variant, the iron-porphyrin moiety of **1-Fe** is sandwiched between the two subdomains of the protein (Figures 4 and 5), which could then cause a steric hindrance that both makes more difficult the access of the substrate to the iron and induce a stereoselectivity in the transfer of the oxygen atom on the sulfur atom of thioanisole. In such a way, a very reduced part of the protein partner constitutes the asymmetric environment around the catalyst. Additionally, figures 4 and 5 show that the iron-porphyrin moiety is also widely exposed to the solvent, this may explain why the control of the access of the thioanisole substrate to the iron is not very high and why the enantiomeric excess in S-sulfoxide is only moderate.

This enantiomeric excess can be compared to those obtained for this type of reaction in the presence of various artzymes (Table 4). Several artzymes, were found to catalyze the stereoselective sulfoxidation of thioanisole with moderate to high enantiomeric excesses. For example, the insertion of Cr- and Mn-Salen complexes into apomyoglobin variants, either covalently[9] or by host-guest strategy[15,39] led to ee values between 33 and 60% in favor of the R or the S isomer depending upon the variant. Insertion, by the host-guest strategy, of Fe-corrole into Bovin Serum albumin[14] and an anionic iron-porphyrin, Fe(Tetra-p-carboxylatophenylporphyrin, FeTpCPP), into xylanase A[20] led respectively to 38% and 40% ees in favour of the S isomer whereas the insertion of Microperoxidase 8 into monoclonal anti-microperoxidase 8 antibodies[40] led to a 46% ee in favour of the R isomer. Finally, the best ee (93%) in favor of the S isomer, was reported for the oxidation of thioanisole by the vanadyl ion $VOSO_4$ inserted into (strept)avidin[23].

Table 4. Comparative table of yields and enantioselectivity induced by the protein with other systems described in the literature for the sulfoxidation of thioanisole.

Protein	Metal complex	Strategy	ee(%)	Conf.	Ref.
NCS-3.24 variant	**1-Fe**	Trojan Horse	13	S	This work
anti-œstradiol Antibody 7A3	Fe-anionic porphyrin	Trojan Horse	10	S	26
anti-œstradiol Antibody 7A3	Fe-cationic Porphyrin	Trojan Horse	8	S	24
(strept)avidin	Mn-Salen-biotin	Trojan Horse	11	R	38
Apomyoglobin Variants	Cr-Salen	Host-guest	5-33	R/S	15
Xylanase A	Fe-anionic porphyrin	Host-guest	40	S	20
Apomyoglobin variants	Mn-Salen	Host-guest	60	S	39
Bovin Serum albumin	Fe-Corrole	Host-guest	38	S	14
Anti-MP8 - antibody 3A3	Micropero-xidase 8	Host-guest	46	R	40
(strept)avidin	$VOSO_4$	Covalent	93	S	23
Apomyoglobin variants	Mn-Salen	Covalent	12-51	S	9

At the opposite, all the artzymes produced by the "Trojan Horse" reported until now lead to low enantiomeric excesses. Indeed, Fe-anionic porphyrin-estradiol[26] and Fe-cationic porphyrin-estradiol[24] complexes associated with a monoclonal anti-estradiol antibody only led to 10% and 8% enantiomeric excess in favor of the S isomer whereas a Mn-Salen-biotin-(strept)avidin biohybrid only led to a 11% enantiomeric excess in favor of the R isomer.[38] Since **1-Fe**-NCS-3.24 also leads to a weak enantiomeric excess, it is clear that the "Trojan Horse" strategy may not be the best one to get a high enantioselectivity in the sulfoxidation of thioanisole, using a rather bulky iron-porphyrin as catalyst. This could be related to a bad control of the access of the substrate to the metal center, which could be due to the fact that the metal cofactor stands outside the binding site of the protein.

Conclusion

The aforementioned results describe the synthesis and the characterization of a new anionic metalloporphyrin-testosterone conjugates **1-Fe**. In order to generate new artificial metalloenzymes following the so-called "Trojan horse strategy", this molecule was further associated to a neocarzinostatin variant, NCS-3.24, that was previously engineered using a directed evolution approach for the binding of testosterone. UV-visible spectroscopic studies showed some slight modifications in the spectrum of **1-Fe** in the presence of the NCS-3.24 protein – namely a slight increase in absorbance intensity together with slight 4-5 nm shifts of its characteristic bands- that were in agreement with a change of the surrounding hydrophobicity of the porphyrin and a possible coordination of a weak ligand coming from one amino acid side chain of the protein on one face of the iron. Such observations were clearly in favor of an insertion of the 1-Fe cofactor in the binding site of the NCS-3.24 protein. These studies also allowed the determination of a K_D value of 1.6 µM for the **1-Fe**-NCS-3.24 variant complex (Table 1), that

appeared to be better than those reported for the NCS-3.24-testosterone and -testosterone-hemisuccinate (THS) complexes.[29] Since NCS-3.24 also bound Fe-TpSPP with a K_D of 12.5 μM, it made it clear that a synergetic effect between the binding of the testosterone moiety and that of the porphyrinic ring led to a better association of **1-Fe** with NCS-3.24 than that of both testosterone and THS alone.

Consequently, the requirements to use the **1-Fe**-NCS-3-24 artzyme as a biocatalyst for oxidation reactions in water appeared to be fulfilled, and it was then tested as biocatalyst for the oxidation of thioanisole by hydrogen peroxide. In the presence of **1-Fe**-NCS-3.24, the reaction appeared to be highly chemoselective -no sulfone could be detected- and only led to the sulfoxidation of thioanisole by hydrogen peroxide with a low enantiomeric excess of about 13%. This ee was comparable to those obtained with other artzymes generated following the "Trojan horse" strategy, but lower than those obtained with artzymes based on other approaches, *i.e.* insertion of metal cation or covalent attachment of a metal cofactor in a protein or host-guest strategy (Table 3).

In order to better explain both the binding of **1-Fe** in the cavity of the NCS variant and the resulting stereoselectivity of the sulfoxidation reaction, molecular modelling was performed.

Protein-ligand docking calculations predict a good complementarity between the Trojan horse porphyrin **1-Fe** and the NCS-3.24 variant. As a whole, the calculations agree with the experimental data in particular in predicting better binding with respect to the unsubstituted porphyrin **Fe-TpSPP** and the possibility of a weak direct coordination between the metal and the backbone carbonyl of the phenylalanine Phe 78 of the protein. The iron-porphyrin moiety of **1-Fe** appears to be sandwiched between the two subdomains of the protein (Figures 4 and 5), which could explain the stereoselectivity observed in the sulfoxidation of thioanisole. However the large dimension of the Trojan horse lead to a complete occupancy of all the available cavities of the NCS and results also in a metal vicinity exposed to the solvent. These two aspects could explain why the control of the access of the thioanisole substrate to the iron is not very high and that the enantiomeric excess in S-sulfoxide is only moderate.

Protein-ligand dockings show good complementarities between the Trojan horse and the receptor and confirm that the strategy followed in this work is valid. However, the steroid group used as the Trojan horse element has not maintained in original location but has been slightly displaced toward the superficial space of the receptor. It appears that porphyrin and steroid moieties only seem to sum strong hydrophobic interactions with the protein with only residual polar contacts too. This suggests that the specificity of the receptor for any of the chemical groups (both characterized at tens of □M) is too low for one of them dictating the geometric feature of the final system. Therefore, this study sheds light on the limitation of the applicability of the so-called "Trojan Horse" strategy. Without a strong affinity of the chemical used as a template for the receptor, foreseeing the geometrical features of active artificial metalloenzymes is hazardous. In our case, whether the steroid has some role in guiding the binding process is still unclear.

It is then likely that increasing the interaction of the metal cofactor with the protein could lead to better enantioselectivities. The synthesis of new cofactors in which the distance between the metal complex and the testosterone anchor will be shorter will then be undertaken. This could be achieved either by directly substituting the testosterone moiety on one *meso*-carbon of the porphyrin ring, or alternatively by substituting the porphyrin ring with a smaller ligand such as salen for example.

Experimental Section

Physical measurements. UV-visible spectroscopy studies were performed on double beam UVIKON 860XL and CARY 300BIO VARIAN spectrophotometers. ^{1}H NMR and ^{13}C NMR spectra were recorded on BRUKER AM 250, 300, 360 spectrometers.

Synthesis of free base 5,10,15-Tris(p-sulfonatophenyl)-20-(p-aminophenyl)porphyrin ($TpSPpNH_2PPH_2$) : 5,10,15-Tris(p-sulfonatophenyl)-20-(p-aminophenyl)porphyrin (**$TpSPpNH_2PPH_2$**) was prepared in two steps as described previously.[26] The nitration of tetraphenylporphyrin by $NaNO_2$ was first carried out according to the method described by Smith and coll.,[32] followed by the reduction of the nitro group by $SnCl_2$.[33] The sulfonation of the obtained 5,10,15-phenyl-20-*p*-aminophenylporphyrin was then carried out according to the method described by Fleischer et al.[34]

Synthesis of 17'-succinimidyltestosterone: The synthesis of 17'-succinimidyl-testosterone was inspired from the work of Hong Xu Chen and Xin Xiang Zhang.[31] A solution of testosterone (580 mg, 2 mmol) and succinic anhydride (2.2 g, 22 mmol.) in 20 mL anhydrous pyridine, was stirred for 12 hours at 110 °C. The reaction mixture was cooled down at RT. 25 mL of water were then added and a saturated solution of $NaHCO_3$ was further added until pH 12 was reached. The mixture was then washed three times with 20 mL of diethyl ether. The aqueous layer was acidified by addition of 1 M HCl until a white precipitate was observed and was then extracted three times with 20 mL of diethyl ether. The organic layers were combined, dried over anhydrous $MgSO_4$, and filtered. The filtrate was then concentrated under reduced pressure and 17'-succinimidyltestosterone (571 mg) was obtained as white crystals (73% yield). $\mathbf{R_f}$ = 0.5 in CH_2Cl_2/MeOH, 90/10; **^{1}H NMR** ($CDCl_3$, 250 MHz, δ(ppm)): 9.55 (m, 1H, OH), 5.66 (s, 1H, H4'), 4.52 (t, 1H, H17'), 2.5 (m, 4H, H1 and H2), 1.16-2.71 (m, 20 H), 1.45 (s, 3H, CH_3), 0.81 (s, 3H, CH_3); **^{13}C NMR** ($CDCl_3$, 90 MHz, δ(ppm)) : 199.6 (C3'), 176.2 (C=O), 171.4 (C=O), 123.1 (C4'), 82.3 (C17'), 42.1 (C13'), 38.1 (C19'), 36.0 (C2'), 22.9 (C11'), 19.9 (C15'), 16.8 (CH_3), 11.4 (CH_3); **ESI [M+H$^+$]** 389.05 (Exact mass = 388.22 g.mol^{-1}).

Synthesis of 5,10,15-tris(p-sulfonatophenyl)-20-(4-phenyl(17'-O-succinimidyltesto-sterone))porphyrin ($TpSPpNHSucTestoPPH_2$) 1: A solution of 17'-succinimidyltestosterone (130 mg, 0.345 mmol, 1 equiv.) and *N*-methyl morpholine (0.2 mL) in 5 mL anhydrous THF was cooled down in an ice bath. Isobutyl chloroformate (0.2 mL) was added and the mixture was stirred at −5 °C for one hour. $TpSPpNH_2PPH_2$ (300 mg, 0.345 mmol) was then added and the mixture was heated at 90°C under argon for 12 hours. The reaction was monitored by TLC. Another 200 mg of activated 17'-succinimidyltestosterone was then added and the reaction mixture was heated at 90 °C overnight. The solvent was then removed under reduced pressure, and the residue was re-dissolved in a minimum amount of distilled water and washed with CH_2Cl_2. Crude **1** was then precipitated as a purple solid with methanol. The solid was dissolved in a minimum amount of water and applied to a Na^+-activated cation exchange column (AG-50W-X8). After lyophilization, **1** was obtained as a powdered purple solid (106 mg, 24% yield). $\mathbf{R_f}$ = 0.6 (AcOEt/ MeOH; 50/50); **UV-Visible :** (H_2O,λ_{max} (nm)) : 415 (Soret), 516, 558, 587, 638; **HRMS (MALDI)** m/z = 1239.34791 [M+3H$^+$] (exact mass = 1239.34 g.mol^{-1})

Synthesis of 5,10,15-tris(p-sulfonatophenyl)-20-(4-phenyl(17'-O-succinimidyltestosterone)) 1 and of its iron(III) complex 1-Fe: The insertion of iron into **1** was achieved by incubating overnight the free base porphyrin (20 mg., 0.015 mmol.) and $FeCl_2.4\,H_2O$ (33 mg., 10 eq.) at 4°C in 20 mL 1M acetate buffer, pH 4 under inert atmosphere.[24] Quantitative insertion of iron into the starting material was confirmed by UV/vis monitoring. When the reaction was over, the crude **1-Fe** was precipitated by addition of acetone. The obtained

solid was filtered and re-dissolved in methanol. After filtration, the solvent was removed under reduced pressure and complex **1-Fe** was obtained as a dark purple solid (20 mg., yield = 95 %). **UV-visible:** λ_{max}(nm) in 50 mM citrate-phosphate buffer,p□.□.□ (nm) : 412 (Soret), 540.

Expression and purification of the neocarzinostatin variant (NCS-3.24): The NCS protein variant NCS-3.24 was prepared as previously reported by of Minard *et al.*[29,30] *E.coli* BLR(DE3) pLysS strain (Novagen) were used as expression host. Cells transformed with the phagemid containing the gene coding for the protein were grown in 500 ml of 2YT medium in a 2 l flask for 70 h at 30 °C, 200 rpm, in the presence of 100 µg/ml ampicillin and 30 µg/ml chloramphenicol. Under these conditions the protein is efficiently secreted. Bacterial pellets were removed by 15 min centrifugation at 9000 **g** and the soluble secreted proteins were precipitated with ammonium sulfate (650 g/l). Precipitated proteins were solubilized in TBS, and desalted by overnight dialysis at 4 °C against TBS. The dialysed extract was cleared from any insoluble material by centrifugation for 20 min at 17,000 **g**.

His-tagged variant protein was purified using a nickel affinity chromatography (Ni-NTA-agarose Qiagen). The protein, eluted in 0.25 M imidazole, was concentrated and injected in a size-exclusion chromatography column (Hiload™ 16/60 Superdex™ 75) previously equilibrated with 25 mM Tris (pH 7.5) buffer. The purity of the final sample was checked with an overloaded SDS-PAGE gel, which had to show one well-resolved band with no visible contamination.The functionality of the purified proteins was checked by ELISA as described,[28] with 50 nM protein. A Maxisorp ELISA plate (Nunc) was coated with streptavidin–biotinylated testosterone complex. Bound proteins were detected with an anti-His6-tag horseradish peroxidase conjugated monoclonal antibody (Roche Diagnostics). TBS, streptavidin and BSA coated wells were used as negative controls. Proteins were also incubated in the presence of a free competitor (100 □M and 1 mM testosterone hemisuccinate (THS)) to check the specificity of the testosterone binding**.**

Characterization of the iron(III)-porphyrin-NCS-3.24 variant complex: comparison of the UV–vis spectrum of the iron(III)-porphyrin cofactor, 1-Fe, with that of the corresponding iron(III)-porphyrin-NCS-3.24 complex: A 5 µM solution of **1-Fe** in 50 mM citrate-phosphate buffer, pH 4**,** was prepared by mixing 25 µL of a 100 µM solution of **1-Fe** and 475 µL of 0.05 M phosphate-citrate buffer pH 4. In parallel, a 5 µM solution of **1-Fe-**NCS-3.24 in 50 mM phosphate–citrate buffer pH 4**,** was obtained by mixing 25 µL of a 100 µM solution of **1-Fe** and 10 µL of a 305 µM solution of NCS-3.24 (1.2 eq.) in 465 µL of 50 mM phosphate-citrate buffer pH 4. The UV–visible spectra of those solutions were then recorded between 300 and 750 nm.

Titration of the NCS-3.24 variant by the 1-Fe cofactor, and determination of the dissociation constant of the 1-Fe-NCS-3.24 complex: Increasing amounts (from 0 to 1.2 molar equivalents, final concentration of the protein in the 0.24 - 5.9 µM range) of a 305 µM solution of NCS-3.24 were added to a 5 µM solution of **1-Fe** in a 50 mM citrate-phosphate buffer, pH 4. The absorbance of the solution A_s was recorded between 250 and 750 nm, 5 min after each addition. The same experiment was performed to measure the absorbance A_1 of the cofactor alone. After correction of the dilution induced by the volume of cofactor added, the difference $\Delta A = A_1 - A_s$ at 412 nm was plotted as a function of the number of equivalents of NCS-variant added.

K_D values were then determined by an already described method [19b] from the non-linear regression of the curve representing the initial concentration of NCS variant $[NCS_v]_0$ as a function of $\Delta A/(\varepsilon_{\underline{1\text{-}Fe}} - \varepsilon_{\underline{1\text{-}Fe}\text{-}NCS_v}v$ at 412 nm; where: $\Delta A = A_1 - A_s$ at 412 nm; $[NCS_v]$ stands for the concentration of NCS variant : NCS-3.24, and [**1-Fe**-NCS_v] for the concentration of NCS3-24-**1-Fe** complex formed.

Sulfoxidation of thioanisole by H_2O_2 Catalyzed by 1-Fe and the 1-Fe–NCS-3.24 variant complex : The NCS variant (7.5 µM) was incubated for two hours at room temperature with **1-Fe** (5 µM) in 412.5 mL 50 mM citrate-phosphate buffer, pH 4. 12.5 µL of a 0.1 M solution of thioanisole in acetonitrile (Final concentration: 2.5 mM) and 25 µl of a 0.01 M solution of imidazole in bi-distilled water (Final concentration: 500 µM) were then added. The oxidant, H_2O_2 (final concentration, 2.5 mM), was then added to the solution at a rate of 5 x 5 µL drops of 0.5 mM H_2O_2 over a period of 1 h. The same procedure was followed with the cofactor alone, and without cofactor. The organic products were extracted twice with ethyl-acetate and analyzed on a Thermo electron FOCUS GC equipped with a TR-5 7 mm x 0.32 mm column, using benzophenone as the internal standard to determine the degree of conversion of the sulfide.

The organic layer was then concentrated under reduced pressure and the residue was re-dissolved in a minimum amount of isopropanol before being analyze on a Perkin Elmer HPLC equipped with a chiral Chiracel OD-H column to determine the enantiomeric excess of the sulfoxide obtained. The eluant was isohexane/propan-2-ol; 95/5 v/v, and the flow rate was 1 $mL.min^{-1}$.

Molecular Modelling: Protein-ligand docking experiments have been performed using the program GOLD (version 5.1).[41] Calculations have been performed on the X-ray structure of the 3-tes-24 variant of the NCS.[29] Because of the wide exposure of the binding site of this enzyme, calculations were performed without rotameric flexibility of its residues, avoiding in such a way major false positives. However, three key water molecules characterized in the same environment have been considered in the calculations: 2047, 2096 and 2116. These molecules were allowed to be rotated or eventually removed during the docking cycles.

For each system, 20 docking solutions have been generated. Calculations have been performed using a cavity consistent with the location of the ligand in the experimental structure and involving a 20 Å radius sphere radius centred on an atom close to the centre of mass of the binding site. Test calculations on the validity of the scoring functions were performed using the four energetic schemes of GoldScore,[41] GOLD,[42] Chemscore[43] and ChemPLP.[44] They were benchmarked in function of their ability to reproduce both testosterone sites observed in the crystal structures. And atom type optimized in house to account for possible coordination binding of the metal with nearby residues was used for the iron.[45]

The ligands have been prepared using 1) the X-ray structure of the steroid further minimized under the GAFF force field in the UCSF Chimera environment,[46] 2) a DFT minimized structure of the naked porphyrin as reported previously[20] and 3) a minimized structure of the Trojan were both 1 and 2 were bridged together with the linker synthesized experimentally. Analysis and graphic rendering were generated under the UCSF Chimera environment.

Acknowledgements

The authors would like to thank the "Agence Nationale de la Recherche" (ANR REBAR, ANR CATHYMETOXY).

Notes and references

[a] Institut de Chimie Moléculaire et des Matériaux d'Orsay, UMR 8182 CNRS, Laboratoire de Chimie Bioorganique et Bioinorganique, Bât. 420, Université Paris-sud, 91405 Orsay Cedex (France) E-mail: Jean-Pierre.mahy@u-psud.fr.

[b] Institut de Biochimie et de Biophysique Moléculaire et Cellulaire, UMR 8619 CNRS, laboratoire de Modélisation et d'Ingénierie des Protéines, Bât 430, Université Paris XI, 91405 Orsay Cedex (France).
[c] Departament de Química, Universitat Autònoma de Barcelona, Edifici C.n., 08193 Cerdonyola del Vallès, Barcelona (Spain).

Keywords: Artificial metalloenzyme · Trojan horse · Porphyrin · Sulfoxidation · Molecular modeling

1 Q. Raffy, R. Ricoux and J-P. Mahy, in *Focus on Catalysis Research: New Developments,* ed. M. Ghang and B. Ramel, Nova Science publishers Inc., New York, 2011, pp. 31-62; T. R. Ward, *Acc. Chem. Res*., 2011, **44**, 47-57.
2 T. Kokubo, T. Sugimoto, T. Uchida, S. Tanimoto and M. Okano, *J. Chem. Soc., Chem. Commun.,* 1983, **14**, 769-770.
3 C. Bertucci, C. Botteghi, D. Giunta, M. Marchetti and S. Paganelli, *Adv Synth Catal.,* 2002, **344**, 556-562; M. Marchetti, G. Mangano, S. Paganelli and C. Botteghi, *Tetrahedron Lett.* 2000, **41**, 3717-3720.
4 F. van de Velde, L. Könemann, F. van Rantwijk and R. A. Sheldon, *Chem. Commun.,* 1998, **17**, 1891-1892; C. Esmieu, M. V. Cherrier, P. Amara, E. Girgenti, C. Marchi-Delapierre, F. Oddon, M. Iannello, A. Jorge-Robin, C. Cavazza, and S. Ménage, *Angew. Chem. Int. Ed.,* 2013, **52**, 3922-3925.
5 K. Okrasa and R. J. Kazlauskas, *Chem. Eur. J.*, 2006, **6**, 1587-1596; A. Fernández-Gacio, A. Codina, J. Fastrez, O. Riant, P. Soumillion, *ChemBioChem.,* 2006, **7**, 1013-1016.
6 D. Coquière, J. Bos, J. Beld and G. Roelfes, Angew. *Chem. Int. Ed.,* 2009, **48**, 5159-5162.
7 S. M. Pratter, C. Konstantinovics, C. M. Di Giuro, E. Leitner, D. Kumar, S. P. de Visser, G. Grogan and G. D. Straganz, *Angew. Chem. Int. Ed.,* 2013, **52**, 9677-9681.
8 R. R. Davies and M. D. Distefano, *J. Am. Chem. Soc.,* 1997, **119**, 11643-11652.
9 J. R. Carey, S. K. Ma, T. D. Pfister, D. K. Garner, H. K. Kim, J. A. Abramite, Z. Wang, Z. Guo, Y. Lu, *J. Am. Chem. Soc.,* 2004, **126**, 10812-10813.
10 M. T. Reetz, *Tetrahedron,* 2002, **58**, 6595-6602.
11 M. T. Reetz, M. Rentzsch, A. Pletsch, M. Maywald, P. Maiwald, J. P. Peyralans, A. Maichele, Y. Fu, N. Jiao, F. Hollmann, R. Mondiere, A. Taglieber, *Tetrahedron,* 2007, **63**, 6404-6414.
12 L. Panella, J. Broos, J. Jin, M. W. Fraaije, D. B. Janssen, M. Jeronimus-Stratingh, B. L. Feringa, A. J. Minnaard, J. G. de Vries, *Chem Commun., (Camb)* 2005, **45**, 5656-5658.
13 B. Talbi, P. Haquette, A. Martel, F. de Montigny, C. Fosse, S. Cordier, T. Roisnel, G. Jaouen, M. Salmain, *Dalton Trans.*, 2010, **39**, 5605-5607; M. V. Cherrier, S. Engilberge, P. Amara, A. Chevalley, M. Salmain, J. C. Fontecilla-Camps, Eur. J. Inorg., Chem., 2013, **21**, 3596-3600.
14 A. Mahammed, Z. Gross, *J. Am. Chem. Soc.,* 2005, **127**, 2883-2887.
15 M. Ohashi, T. Koshiyama, T. Ueno, M. Yanase, H. Fujii, Y. Watanabe, *Angew. Chem., Int. Ed.,* 2003, **9**, 1005-1008; T. Ueno, T. Koshiyama, M. Ohashi, K. Kondo, M. Kono, A. Suzuki, T. Yamane, Y. Watanabe, *J. Am. Chem. Soc.,* 2005, **127**, 6556-6562; T. Ueno, T. Koshiyama, S. Abe, N. Yokoi, M. Ohashi, H. Nakajima, Y. Watanabe, *J. Organomet. Chem.,* 2007, **692**, 142-147.
16 M. T. Reetz, N. Jiao, *Angew. Chem. Int. Ed. Engl*., 2006, **45**, 2416-2419.
17 T. Matsuo, A. Asano, T. Ando, Y. Hisaeda and T. Hayashi, *Chem. Commun.*, 2008, **31,** 3684-3686.
18 T. Hayashi, Y.Hisaeda, *Accounts Chem. Res.,* 2002, **35**, 35-43; H. Sato, T. Hayashi, T. Ando, Y. Hisaeda, T. Ueno and Y Watanabe, *J. Am. Chem. Soc.,* 2004, **126**, 436-437; T. Hayashi, D. Murata, M. Makino, H. Sugimoto, T. Matsuo, H. Sato, Y. Shiro and Y. Hisaeda, *Inorg. Chem.,* 2006, **45**, 10530-10536; T. Matsuo, D. Murata, Y. Hisaeda, H. Hori and T. Hayashi, *J. Am. Chem. Soc.* 2007, **129**, 12906; T. Matsuo, A. Hayashi, M. Abe, T. Matsuda, Y. Hisaeda and T. Hayashi, *J. Am. Chem. Soc.,* 2009, **131**, 15124.
19 T. Matsuo, T. Tsuruta, K. Maehara, H. Sato, Y. Hisaeda and T. Hayashi, *Inorg. Chem., 2005,* **44**, 9391-9396; K. Kano, H. Kitagishi, C. Dagallier, M. Kodera, T. Matsuo, T. Hayashi, Y. Hisaeda and S. Hirota, *Inorg. Chem.,* 2006, **45,** 4448-4460; T. Matsuo, T. Ikegami, H. Sato, Y. Hisaeda and T. Hayashi, *J. Inorg. Biochem.,* 2006,**100**, 1265-1271; K.Harada, M. Makino, H. Sugimoto, S. Hirota, T. Matsuo, Y. Shiro, Y. Hisaeda and T.Hayashi, *Biochemistry*, 2007, **46,** 9406-9416; T. Matsuo, K. Ito, Y. Nakashima, Y. Hisaeda and T. Hayashi, *J. Inorg. Biochem.,* 2008, **102,** 166-173.
20 R. Ricoux, M. Allard, R. Dubuc, C. Dupont, J-D. Marechal, J-P. Mahy, *Org. Biomol. Chem.,* 2009**,** 7, 3208-3211.
21 M. Allard, C. Dupont, V. Munoz-Robles, N. Doucet, A. Lledos, J-D. Marechal, A. Urvoas, J-P. Mahy, R. Ricoux, *ChemBioChem.,* 2012 **;** ***13***, 240-251.
22 J. Collot, J. Gradinaru, N. Humbert, M. Skander, A. Zocchi, T. R. Ward, *J. Am. Chem. Soc*., 2003, **125**, 9030-9031; (b) C. Letondor, T. R. Ward, *ChemBiochem.* 2006, **7**, 1845-1852.
23 A. Pordea, M. Creus, J. Panek, C. Duboc, D. Mathis, M. Novic, T. R. Ward, *J. Am. Chem. Soc.,* 2008, **130**, 8085-8088.
24 Q. Raffy, R. Ricoux, J-P. Mahy, *Tetrahedron Lett.* 2008, **49**, 1865-1869.
25 Q. Raffy, R. Ricoux, E. Sansiaume, S. Pethe, J-P. Mahy, *J. Mol. Catal. A: Chem.* 2010, **317**, 19-26.
26 E. Sansiaume, R. Ricoux, D. Gori, J-P. Mahy, *Tetrahedron: Asymmetry,* 2010, ***21***, 1593-1600.
27 N. Izadi-Pruneyre, E. Quiniou, Y. Blouquit, J. Perez, P. Minard, M. Desmadril, J. Mispelter, A. Adjadj, *Protein Science,* 2001, **10**, 2228-2240.
28 B. Heyd, F. Pecorari, B. Collinet, E. Adjadj, M. Desmadril, P. Minard, *Biochemistry*, 2003, **42,** 5674-5683.
29 A. Drevelle, M. Graille, B. Heyd, I. Sorel, N. Ulryck, F. Pecorari, M. Desmadril, H. van Tilbeurgh, P. Minard, *J. Mol. Biol.,* 2006, **358**, 455-471.
30 A. Drevelle, A. Urvoas, M. Ben Hamida-Rebaï, G. Van Vooren, M. Nicaise, M. Valerio-Lepiniec, M. Desmadril, Ch. H. Robert, P. Minard, *ChemBioChem.,* 2009, **10,** 1349-1359.
31 H. X. Chen, X.X. Zhang, *Electrophoresis*, 2008, **29**, 3406-3413.
32 R. Luguya, L. Jaquinod, F.R. Fronczek, M. Graça, H. Vicente, K. M. Smith, Tetrahedron, 2004 , **60** 2757-2763.
33 J.P. Collman, R.R. Gagne, C.A. Reed, T.R Halbert, G. Lang, W.T. Robinson, J. Am. Chem. Soc., 1975 **97** 1427-1439.
34 E. B. Fleischer, J. M. Palmer, T. S. Srivastava, A. Chatterjee, *J. Am. Chem. Soc.,* 1971, ***93***, 3162-3167.

35 R. Ricoux, H. Sauriat-Dorizon, E. Girgenti, D. Blanchard, J-P. Mahy, *J. Immunol. Meth.,* 2002, **269**, 39–57.
36 (a) L. Casella, M. Gullotti, R. Ghezzi, S. Poli, T. Beringhelli, S. Colonna, G. Carrea, *Biochemistry*, 1992, ***31***, 9451-9459. (b) S. Colonna, N. Gaggero, G. Carrea, P. Pasta, *J. Chem. Soc. Chem. Commun.* 1992, **4,** 357-358; (c) K. Okrasa, E. Guibé-Jampel, M. Thérisod, *J. Chem. Soc., Perkin Trans. 1* 2000, 1077-1079.
37 J.Y. Liu, X.F. Li, Y.Z. Li, W.B. Chang, A.J. Huang, *J. Mol. Catal., A* 2002, **187**, 163-167.
38 A. Pordea, D. Mathis, T. R. Ward, J. Organomet. Chem., 2009**, 694**, 930-936.
39 J. L. Zhang, D. K. Garner, L. Liang, Q. Chen, Y. Lu, Chem. Commun., 2008, 1665-1867.
40 R. Ricoux, E. Lukowska, F. Pezzotti, J. P. Mahy, *Eur. J. Biochem.,* 2004, **271**, 1277-1283;.
41 M. L. Verdonk, J. C. Cole, M. J. Hartshorn, C. W. Murray, R. D. Taylor, *Proteins*, 2003, **52**, 609.
42 W. T. M. Mooij, M. L. Verdonk, *Proteins*, 2005, **61**, 272.
43 M. D. Eldridge, C. W. Murray, T. R. Auton, G. V. Paolini, *J. Comput.-Aided Mol. Des.,* 1997, **11**, 425; C. W. Murray, T. R. Auton, M. D. Eldridge, *J. Comput.-Aided Mol. Des.,* 1998, **12**, 503.
44 O. Korb, T. Stützle, T. E. Exner, *J. Chem. Inf. Model.,* 2009, **49**, 84.
45 V. M. Robles, E. Ortega-Carrasco, E. G. Fuentes, A. Lledós, J.-D. Maréchal, *Faraday Discussions,* 2011, **148**, 137.
46 E. F. Pettersen, T. D. Goddard, C. C. Huang, G. S. Couch, D. M. Greenblatt, E. C. Meng, T. E. Ferrin, *J. Comput. Chem*., 2004**, 25**, 1605-1612.

Enantioselective sulfoxidation of sulfides by H_2O_2 catalysed by an artificial metalloenzyme :

Table of contents entry:

Following the Trojan-Horse strategy, a new artificial metalloenzyme, obtained by non-covalent insertion of an anionic Fe-porphyrin–testosterone conjugate into the neocarzinostatin NCS-3.24 variant, catalysed the enantioselective sulfoxidation of thioanisole by H_2O_2.